HHS Public Access

Author manuscript

Oncogene. Author manuscript; available in PMC 2024 March 01.

Published in final edited form as:

Oncogene. 2018 July ; 37(27): 3672–3685. doi:10.1038/s41388-018-0156-9.

Novel bone morphogenetic protein receptor inhibitor JL5 suppresses tumor cell survival signaling and induces regression of human lung cancer

Jenna H. Newman[1], **David J. Augeri**[2], **Rachel NeMoyer**[3], **Jyoti Malhotra**[4], **Elaine Langenfeld**[5], **Charles B. Chesson**[1], **Natalie S. Dobias**[1], **Michael J. Lee**[3], **Saeed Tarabichi**[3], **Sachin R. Jhawar**[6], **Praveen K. Bommareddy**[1], **Sh'Rae Marshall**[1], **Evita T. Sadimin**[7], **John E. Kerrigan**[8], **Michael Goedken**[9], **Christine Minerowicz**[7], **Salma K. Jabbour**[6], **Shengguo Li**[1], **Mary O. Carayannopolous**[7], **Andrew Zloza**[#1,3], **John Langenfeld**[#5]

[1]Section of Surgical Oncology Research, Division of Surgical Oncology, Rutgers Cancer Institute of New Jersey, New Brunswick, NJ 08903, USA

[2]Office of Translational Science, Molecular Design and Synthesis, Rutgers, The State University of New Jersey, Piscataway, NJ 08854, USA

[3]Department of Surgery, Rutgers Robert Wood Johnson Medical School, Rutgers, The State University of New Jersey, New Brunswick, NJ 08903, USA

[4]Division of Medical Oncology, Rutgers Cancer Institute of New, Jersey, New Brunswick, NJ 08903, USA

[5]Department of Surgery, Division of Surgical Oncology and Thoracic Surgery, Rutgers Cancer Institute of New Jersey, New Brunswick, NJ 08903, USA

[6]Department of Radiation Oncology, Rutgers Robert Wood Johnson Medical School, New Brunswick, NJ 08903, USA

[7]Department of Pathology and Laboratory Science, Rutgers Robert Wood Johnson Medical School, New Brunswick, NJ 08903, USA

[8]Department of Bioinformatics, Rutgers Biomedical Health Sciences, Rutgers, The State University of New Jersey, Piscataway, NJ 08854, USA

[9]Office of Translational Science, Research Pathology Services, Rutgers, The State University of New Jersey, Piscataway, NJ 08854, USA

Andrew Zloza andrew.zloza@rutgers.edu.

These authors contributed equally: Andrew Zloza and John Langenfeld.

Author contributions: J.L. and A.Z. designed the experiments, interpreted the data, and wrote the manuscript. J.H.N. performed *in vivo* experiments and interpreted the data. D.J.A. designed and synthesized JL5. R.N., E.L., C.B.C., N.S.D., M.J.L., S.T., S.R.J., P.K.B., S.M., and S.L. performed experiments. S.K.J. designed experiments. J.M. performed genetic alternations studies, M.G. interpreted toxicity studies, and M.O.C. performed blood chemistry studies. E.T.S. and C.M. evaluated and interpreted pathology data. J.E.K. designed BMP inhibitors. All authors contributed to writing and/or providing feedback on the manuscript.

Electronic supplementary material The online version of this article (https://doi.org/10.1038/s41388-018-0156-9) contains supplementary material, which is available to authorized users.

Compliance with ethical standards

Conflict of interest J.L., D.J.A., and J.E.K. are inventors of pending patents related to this study. The remaining authors declare that they have no conflict of interest.

[#] These authors contributed equally to this work.

Abstract

BMP receptor inhibitors induce death of cancer cells through the downregulation of antiapoptotic proteins XIAP, pTAK1, and Id1-Id3. However, the current most potent BMP receptor inhibitor, DMH2, does not downregulate BMP signaling in vivo because of metabolic instability and poor pharmacokinetics. Here we identified the site of metabolic instability of DMH2 and designed a novel BMP receptor inhibitor, JL5. We show that JL5 has a greater volume of distribution and suppresses the expression of Id1 and pTak1 in tumor xenografts. Moreover, we demonstrate JL5-induced tumor cell death and tumor regression in xenograft mouse models without immune cells and humanized with adoptively transferred human immune cells. In humanized mice, JL5 additionally induces the infiltration of immune cells within the tumor microenvironment. Our studies show that the BMP signaling pathway is targetable in vivo and BMP receptor inhibitors can be developed as a therapeutic to treat cancer patients.

Introduction

An estimated 170,000 people this year in the U.S. will die from lung cancer. More people will die from lung cancer then prostate, colon, breast, and kidney cancer combined. Despite advances in targeted therapy 85% of patients diagnosed with lung cancer will succumb to the disease. It is clear that better treatment options are needed for the treatment of lung cancers.

Bone morphogenetic proteins (BMPs) are members of the transforming growth factor beta (TGFβ) superfamily that are phytogenetically conserved morphogens required for embryonic development across species from insects to humans [1, 2]. BMP2 and BMP4 regulate a plethora of activities during embryogenesis, including the development of the lung. Following the development of the lungs there is little expression of BMP signaling in normal adult lung tissue [1]. The BMP signaling cascade is reactivated in lung cancer and inflammation [1, 3]. Studies have reported that the bone morphogenetic signaling cascade has a significant role in promoting tumorigenesis in lung and other cancers. The BMP2 ligand is overexpressed in 98% of non-small cell lung cancers but not in benign lung tumors [4]. BMP signaling is reported to enhance tumorigenesis in many other cancers including prostate [5], breast [6, 7], pancreas [8], melanoma [9], and sarcoma [10]. Aberrant BMP signaling has been reported to enhance cell migration, invasion, metastasis, proliferation, and angiogenesis, and is associated with a worse prognosis [3, 11–14].

There are ~20 BMP ligands that signal through trans-membrane serine/threonine kinases composed of type I and type II receptors. The type I receptors are ALK2 (ActR-1), ALK3 (BMPR-IA), and ALK6 (BMPR-IB) [15] and the type II receptors are BMPR-II and activin type II receptors ActR-II and AcR-IIB [15]. There are different affinities of the BMP ligands to each type I receptors [15]. Ligand binding to the type I receptor leads to phosphorylation by the constitutively active type II receptor. The BMPRI/BMPRII receptor complex phosphorylates Smad-1/5 [16], which then translocates to the nucleus leading to

the transcription activation of downstream target genes including inhibitor of differentiation proteins (Id1, Id2, and Id3) [17–21].

Recently, we reported that the BMP signaling cascade regulates several antiapoptotic proteins in lung cancer cells through evolutionarily conserved signaling pathways, which include X-linked inhibitor of apoptosis protein (XIAP), TGFβ activated kinase 1 (TAK1), and inhibitor of differentiation proteins (Id1-Id3) [22]. During embryonic development, XIAP binds to the BMP type I and type II receptors preventing its ubiquitination and subsequent degradation via proteasomes, thus increasing its expression [23]. XIAP binds to TAB1, leading to the activation of TAK1 [24]. XIAP is the most potent of the inhibitor of apoptosis proteins and is the only antiapoptotic protein that inactivates caspases [25]. XIAP binds and inactivates effector caspase-3 and caspase-7 and initiator caspase-9 [26]. XIAP has been shown to block apoptosis induced by many pro-apoptotic agents. TAK1 also potently inhibits apoptotic cell death through the activation of NF-kappa B (NF-κB) [27] and prevention of reactive oxygen species (ROS) production [28]. NF-κB inhibition of apoptotic cell death involves the induction of cellular FLICE-like protein (c-FLIP), XIAP, cellular inhibitor of apoptosis protein 1 (c-IAP-1), and c-IAP-2 [27].

Dorsomorphin was identified in a zebrafish library screen to be a small molecule inhibitor of the BMP receptors [29]. Several generations of BMP inhibitors have been synthesized based on substitutions to this pyrazolo[1,5-*a*]pyrimidine core with varying affinities to the kinase domain of the BMP type I and type II receptors [30, 31]. The BMP analog, DMH1 has been shown in tumors in mice to suppress metastatic growth without tumor regression or downregulation of Id1, TAK1, or XIAP [7, 32]. Our in vitro studies showed that the BMP analog DMH2 is significantly more potent in downregulating XIAP, pTAK1, and Id1 expression and inducing death of lung cancer cells than LDN-193189 and DMH1 [22]. However, DMH2 does not downregulate XIAP, ID1, or pTAK1 in tumor xenografts, likely because of its poor pharmacokinetic profile in mice [22]. The development of stable BMP inhibitors that have potent inhibition of BMP-regulated antiapoptotic proteins Id1, pTAK1, and/or XIAP in tumor xenografts is needed to better evaluate the role of BMP inhibitors as a cancer therapeutic. The BMP signaling pathway is also known to regulate the activation and development of dendritic cells [33], T cells [34], and natural killer cells [35]. However, the effects of BMP inhibitors on immune cells within the tumor microenvironment are not known. Since BMP signaling regulates immune cells it essential to understand how BMP inhibitors affect the immune cells within the tumor microenvironment and to determine whether BMP inhibition in the context of an immune system enhances or attenuates tumor growth.

In our study, genetic profiling indicates that mutations that could cause resistance to a BMP receptor inhibitor are infrequent in non-small cell lung cancer (NSCLC). We have identified the chemical instability of DMH2 and designed a compound, JL5, to circumvent the chemical hydrolysis of the morpholine side-chain. JL5 inhibits BMP type I and type II receptors at similar concentrations, induces in vitro cancer cell death, and downregulates Id1, XIAP, and pTAK1 with similar potency as DMH2. Importantly, JL5 is more metabolically stable than DMH2, and downregulates Id1 and pTAK1 and induces tumor regression in lung tumor xenografts. JL5 demonstrates a positive effect on immune

cells within the tumor microenvironment by increasing immune cell infiltration within the tumor. JL5 maintains suppression of tumor growth even in the presence of adoptively transferred immune cells. These data demonstrate that BMP signaling is targetable in NSCLC and propose that targeted suppression of BMP receptors can be developed as a therapeutic drug to treat lung and other cancers.

Results

BMP ligands are frequently overexpressed in NSCLC

In a prior study, we have shown that BMP2 protein is highly overexpressed in 98% of lung cancers (independent of cell type) with little expression in normal lung tissue [4]. However, genetic alteration could cause resistance to a target-specific therapeutic, by alterations that inactivate the signaling pathway, mutations of the receptor that affect its interaction with the small molecule, and amplifications of essential downstream signaling events. Therefore, to determine whether the BMP signaling cascade is a targetable pathway (i.e., it exhibits low mutation frequency), we queried The Cancer Genome Atlas (TCGA) to examine the genetic alterations effecting BMP ligands, receptors, transcription factors, and downstream targets in NSCLC. Only 2 of the 117 lung adenocarcinomas had a deep deletion, missense mutation, or truncating mutation of the BMP2 ligand (Fig. 1a). Sixty-eight percent of lung adenocarcinomas had upregulation of mRNA and 26% had amplification of one or more BMP ligands (Fig. 1a).

Genetic alterations of the BMP signaling cascade are infrequent in NSCLC

Deep deletions, truncating mutations, or missense mutations were present in 8 (6%) of the BMP type I and 4 (3%) of the BMP type II receptors among 135 lung adenocarcinomas examined (Fig. 1b). None of the tumors had mutations in all three of the type I or type II receptors (Fig. 1b) Mutations of Smad-1/5/9 were also infrequent (5%) and never occurred in all three transcription factors (Fig. 1b). Amplification of the downstream BMP targets XIAP, TAK1, and Id1 has the potential to cause resistance to a BMP inhibitor if it upregulates expression. Amplification of XIAP occurred in 0.7%, of TAK1/MAP3K7 in 0%, of Id1 in 6%, of Id2 in 0%, and of Id3 in 2% of lung adenocarcinomas (Fig. 1b).

Similar levels of genetic alterations were identified in squamous carcinoma of the lung and adenocarcinoma lung cancer cell lines (Supplementary Fig. 1 and Supplementary Fig. 2). The low rate of mutations and the redundancy of the BMP signaling cascades suggest that resistance to BMP receptor inhibitors in lung cancer because of genetic alterations is likely to be a rare event.

Design of JL5 improves on the pharmacokinetic profile of DHM2

Based on the inability of DMH2 to downregulate XIAP, ID1, or pTAK1 in vivo [22], we designed a series of DMH2 analogs. The pyrazolo [1,5-*a*] pyrimidine core of the BMP dorsomorphin (Fig. 2a) has been utilized as a heterocyclic core to synthesize BMP inhibitors [36]. Analogs of Dorsomorphin, DMH1, DMH2 [30], and LDN-193189 (LDN) [37] differ in the substitutions made at the R-position of the pyrazolo [1,5-*a*] pyrimidine core (Fig. 2a). We found that after four months, aliquoted samples of DMH2 have decreased potency

to downregulate Id1 expression and induce death of lung cancer cells in vitro (personal observation). Analysis using liquid chromatography-mass spectrometry (LCMS) of a sample of DMH2 stored as a solid in a desiccator for 4 months revealed a phenolic byproduct due to morpholine side-chain hydrolysis (Fig. 2b).

This observation led us to design a compound devoid of an oxygen by replacement with a carbon atom to generate JL5 (Fig. 2c). JL5 was synthesized in simple and convergent fashion by palladium-catalyzed coupling using microwave reactor to couple the brominated pyrazolo[1,5-a] pyrimidine '2' to the borate ester of the morpholine side-chain '3' to generate '1' in 48% yield as a white crystalline solid (Supplementary Scheme 1). An additional substitution of JL5 was made at the R2 position of the core with an imidapyrazole creating JL12 (Fig. 2c).

Using mouse liver microsomes, we demonstrated that the intrinsic clearance of JL5 is 48% lower than that of DMH2 (Table 1). Both JL5 and DMH2 demonstrated high binding to mouse plasma proteins (Table 1). Following a single intravenous administration of JL5 to male BALB/c mice at 2 mg/kg dose, JL5 showed very high plasma clearance (194 mL/min/kg) exceeding normal hepatic clearance, likely due to a high volume of distribution (Vss) of 8.78 L/kg and an elimination half-life of 0.57 h, indicative of high tissue penetration (Table 2). The area under the curve (AUC) was determined to be 1605 h×ng/mL with a C_0/C_{max} of 1282 ng/mL (Table 2). The Vss of DMH2 (0.95 L/kg) was lower than that of JL5 (8.78 L/kg) so its distribution into the tissue is significantly lower than that of JL5 (Table 2). Since the pharmacokinetic properties of JL5 were improved over DMH2, we proceeded with further in vitro and in vivo xenograft studies.

JL5 potently inhibits BMP receptors without inducing toxicity

Towards determining the functional capability of JL5, we determined its half maximal inhibitory concentration (IC50) for inhibiting BMP type I and type II receptors. JL5 demonstrated a single digit nanomolar (nM) IC50 for the BMP type I receptors alk2, alk3, and alk6, which is lower than previously reported for DMH2 (Table 3). Although JL5 only had an approximately 8 μM IC50 for the BMP type II receptor BMPR2, it was similar to that of DMH2 (Table 3). JL12 demonstrated very little inhibition of the BMP type I and type II receptors, and therefore, was used as a negative control in our subsequent studies (Table 3). These studies show that the inhibition of the BMP type I and type II receptors by JL5 is very similar to that of DMH2.

To determine whether JL5 causes toxicity, NSG mice were injected intraperitoneally (IP) with 0, 3 mg/kg, 10 mg/kg of JL5 twice daily for 4 days. Mice showed no evidence of systemic toxicity such as loss of appetite, anorexia, and lethargy. Histological examination of the livers, lungs, and kidneys by a veterinary pathologist did not reveal any evidence of toxicity (Supplementary Fig. 3) or weight loss (Supplementary Fig. 4). Further, a blood chemistry screen revealed no significant difference between mice treated with JL5 or DMSO (Supplementary Table 1). In addition, in our 21-day studies (10 mg/kg of intraperitoneal JL5 twice daily) mice had no signs of toxicity as demonstrated by the lack of anorexia, lethargy, or loss of weight.

JL5 inhibits BMP signaling and induces death of lung cancer cells

To determine whether JL5 inhibition of BMP receptors leads to inhibition of downstream BMP signaling mediators, H1299 lung cancer cells were treated with JL5, JL12 (inactive derivative of JL5), and/or DMSO. JL5 treatment caused a decrease in the expression of Id1 and XIAP (Fig. 3a) in a similar manner as previously reported for DMH2 [22]. Like DMH2, JL5 at lower concentrations caused an increase in the expression of pTAK1, which became undetectable at the highest concentration (Fig. 3a) [22]. JL12 had no effect on the expression of Id1, XIAP, or pTAK1 (Fig. 3b). Since BMP signaling is a direct transcriptional regulator of the Id1 promoter, we examined whether JL5 regulates the Id1 promoter. H1299 cells stably expressing the Id1 promoter regulating the luciferase reporter were treated with JL5. JL5 caused a dose-related decrease in the expression of the Id1-luciferase reporter, while JL12 had no effect (Fig. 3c). Three-day treatment with JL5 induced a significant dose-dependent increase in cell death (Fig. 3d) and a decrease in the number of live H1229 cells (Fig. 3e). JL12 had no effect on either cell death or cell growth of the H1299 cells (Fig. 3d, e). JL5 and DMH2 caused the same amount of cell death at 2.5 μM after 3 days (Fig. 3d). After 7 days, the majority of the H1299 cells treated with JL5 were dead with few live cells remaining in comparison to the DMSO control (Fig. 3f, g). JL5 also suppressed growth of A549 cells, an adenocarcinoma cell line harboring an activating K-Ras mutation (Supplementary Fig. 5). JL5 induced the activation of caspase-3 and cleavage of PARP, suggesting like DMH2, it induces apoptotic cell death (Fig. 3h) [22]. Annexin V staining is frequently used to detect early and late stages of apoptosis. Cells that stain for 7-AAD but not Annexin V are considered to have undergone cell death by necrosis. H1299 cells treated with JL5 for 48 h showed a significant increase in the percentage of cells in late stages of apoptosis as well as necrosis (Fig. 3i) in comparison to the DMSO control. The TUNEL assay demonstrated that JL5 induces DNA double-stranded breaks (DSBs) of H1299 cells (Fig. 3j). The caspase inhibitor Z-VAD-FMK (VAD) partially inhibited JL5-induced cell death, while the RIPI kinase inhibitor necrostatin-1 had no effect (Fig. 3k). These data demonstrate that cell death caused by JL5 occurs in part by inducing apoptosis.

JL5 inhibits tumor growth and induces tumor regression in NSG mice without immune cells

Towards determining whether JL5 exhibits anti-tumor effects in vivo, we first examined whether JL5 downregulates BMP downstream targets in established H1299 tumors in NOD-*scid* IL2Rgamma^{null} (NSG) mice that do not have immune cells. Similar to what was reported for DMH2, JL5 at a lower concentration (3 mg/mL) caused a feedback increase in the expression of Id1 after 4 days (Fig. 4a) [22]. After 4 days, JL5-treated tumors (10 mg/kg) had a decreased protein expression of Id1 and TAK1 but not XIAP (Fig. 4a). DMH2 at similar doses did not downregulate Id1, pTAK1, or XIAP in tumor xenografts [22]. Next, we examined the effects of JL5 (10 mg/mL) on established H1299 tumors in NSG mice treated for 21 days. From the point of maximal tumor growth on treatment day 5, JL5 induced an ~35% regression in tumor size by treatment day 14 followed by a plateau in tumor growth (Fig. 4b, c). During this same period the size of tumors in control-treated mice (DMSO) increased by 13%. No significant differences in the amount of tumor cell death or proliferation were observed in tumors examined after 21 days of treatment (Fig. 4d, e).

JL5 induces the influx of immune cells into the tumor microenvironment and induces tumor regression in immune-reconstituted NSG mice

Since NSG mice do not have immune cells, they accept human donor immune cells without rejection. To investigate the anti-tumor effects of JL5 in the presence of immune cells, NSG mice were reconstituted with HLA-compatible patient-derived immune cells (humanized) and xenografts then established with H1299 cells. After the tumors had reached ~5 mm^2 in size the mice were treated with JL5. JL5 caused a reduction in tumor size in humanized mice treated for 21 days (Fig. 5a). From the point of maximal tumor growth on treatment day 7, JL5 again induced an ~35% regression in tumor size by post-treatment day 12 (Fig. 5a, b). After the tumor regression, the tumors then began to grow, suggesting that the immune cells had a growth-promoting role (Fig. 5a). There were no noteworthy histomorphological differences in cell death by H&E staining (Fig. 5c) but there was a significant reduction in proliferation of tumor cells in mice treated with JL5 (Fig. 5d).

To determine the effect of JL5 treatment on immune cells, we examined the presence of immune cells within the tumors. There were significantly more immune cells within the tumor microenvironment in tumors treated with JL5 in comparison to DMSO controls (Fig. 5e). Quantitative image analysis demonstrated that JL5 induced a 67% increase in CD3+ cells and 80% increase in CD4+ cells in comparison to the DMSO control (Fig. 5f).

JL5 induces tumor necrosis on treatment day 13

Since we did not see cell death after 21 days of treatment despite both the humanized and non-humanized xenografts demonstrating tumor regression after ~13 days of treatment, we repeated the humanized xenograft study but analyzed the tumors after 13 days of treatment with JL5. Again, a significant difference in the size and weight of the tumors of mice treated with JL5 compared to vehicle control was observed (Fig. 6a, b). The amount of tumor regression was equivalent to that seen in the prior experiments on treatment day 15. Histological examination revealed increased necrosis in tumors treated with JL5 compared to controls at this timepoint (Fig. 6c). Two independent pathologists agreed on this finding. Computer-based image analysis using morphometrics software of the H&E slides was used to examine necrosis within the tumor. JL5-treated tumors exhibited twice the number of necrotic cells compared to control tumors (Fig. 6d).

Discussion

Drugs targeting specific receptors are frequently only effective if that receptor has an activating mutation. Activating ROS-1 or epidermal growth factor mutations occur in 1% and 13% of NSCLC, respectively [38]. Targeted therapy is also limited by the deletion of the receptor or development of mutations that are not recognized by the drug [39]. Mutations of downstream effector genes can also render a drug inactive [39]. Our analysis supports that BMP signaling cascade is active in the majority of NSCLCs and genetic alterations are unlikely to induce resistance to small molecules targeting the BMP receptors. Expression of BMP ligands and receptors is highly redundant in NSCLC. Ten different BMP ligands were expressed in NSCLC. All three BMP type I and type II receptors were expressed in all of the NSCLC examined. We have shown that all three of the type I BMP receptors

can effectively induce downstream signaling in lung cancer cell lines [40]. The mutation rate of the BMP receptors is low (<5%) and no tumor had mutations in all three of the type I or type II BMP receptors. The very low incidence of amplification of XIAP, TAK1, or Id1 suggests that these downstream effectors would not provide a mechanism inducing resistance to BMP targeted therapy. Overall, these data suggest that targeting the BMP signaling cascade will not be limited by genetic alterations found in either squamous cell carcinomas or adenocarcinomas of the lung.

There are only a few studies examining the effects of BMP receptor inhibitors in tumor xenografts. The BMP inhibitors most frequently used have been DMH1, DMH2, and LDN. Our studies have shown that DMH2 in vitro is significantly more potent than DMH1 or LDN in decreasing the downstream targets Id1, TAK1, and XIAP and inducing cell death of cancer cells [22]. DMH1 and LDN in tumor xenograft studies reduce metastasis but have not demonstrated tumor regression or significant death of cancer cells [7, 41]. DMH2 has a half-life of only 60 min with a low volume of distribution. Surprisingly, DMH2 causes an increase in Id1 expression in tumor xenografts likely from low level of suppression of BMP signaling allowing for activation of TAK1, which can cause a feed-forward activation of BMP signaling [22]. Substituting a carbon for the oxygen on the morphine side-chain improved the stability of DMH2 and resulted in a new compound, JL5. The potency of JL5 to inhibit BMP receptors and regulate BMP signaling of cancer cells is very similar to that of DMH2. Although the serum half-life was not improved, the volume of distribution was significantly better than that DMH2, which likely contributed to the improved anti-tumor effects seen in our studies. It is likely that further improvements in the pharmacokinetic properties of JL5 and the future development of other potent BMP inhibitors will produce even more pronounced in vivo anti-tumor effects.

We show for the first time that a BMP inhibitor induces tumor regression and causes significant cell death in human tumor xenografts in mice. This was associated with a downregulation of Id1 and TAK1 but not XIAP. The binding of XIAP to the BMP receptors stabilizes XIAP leading to increased expression. XIAP can be stabilized by other pathways, including by binding to survivin and phosphorylation by PI-3 kinase [42]. XIAP is an upstream activator of TAK1, which can phosphorylate Smad-1/5 leading to the activation of BMP signaling [22, 44]. The ability to downregulate XIAP is likely to further inhibit BMP signaling leading to greater cell death. During apoptotic cell death smac is released from the mitochondria, which binds and inactivates inhibitor of apoptosis proteins [43]. Smac mimetics have been designed to bind and inactivate inhibitor of apoptosis proteins IAP-1, IAP-2, and XIAP [44]. Combinational therapies utilizing inhibitors of survivin, PI-3 kinase, or smac mimetics should be explored as a potential strategy to further enhance the downregulation of BMP signaling in cancer cells.

The immune system can induce or inhibit the growth of tumors. In our humanized mouse tumor model the immune cells appeared to have a growth-promoting role. This finding argues the importance of including immune cells in preclinical tumor xenograft models to better delineate therapeutic strategies to treat cancer. Importantly, despite the growth-promoting effect of immune cells, JL5 still caused tumor regression. However, tumor regression was not sustained in the presence of immune cells. Surprisingly, only in tumors

with immune cells did JL5 decrease proliferation of cancer cells. Immune cells are known to secrete BMP ligands [45]. An increase in the number of immune cells secreting BMP ligands could enhance the proliferation of tumor cells and suppress the cytotoxic effects of JL5. A more potent BMP receptor inhibitor with a longer duration of action may be able to counter act the growth-promoting effects of immune cells. A potential strategy that could be utilized is to activate cytotoxic immune cells that have become 'exhausted'. Inhibitors of the immune blockade have demonstrated sustained tumor regression in lung and other tumors [46, 47]. However, the response rate is only 20%. The presence of immune cells within the tumor microenvironment is reported to be the best predictor of PD-L1 blockade inducing a response [48]. Further studies are needed to determine whether the enhanced influx of immune cells induced by BMP receptor inhibition can be used to enhance the effects of immunotherapy directed at PD-1 or PD-L1.

BMP signaling is active in the majority of lung cancers and genetic mutations in NSCLC are unlikely to mitigate the effects of BMP receptor inhibitors. The development of JL5 provides a useful tool to examine the mechanisms in vivo by which the BMP signaling regulates the survival of cancer cells and to develop therapeutic strategies. Since JL5 induces the influx of immune cells into the tumor microenvironment, without causing their death, raising the possibility it can be used in conjunction with checkpoint inhibitors. These studies demonstrate that BMP signaling is growth-promoting in cancer, but is targetable supporting the need for further drug development and design of therapeutic strategies.

Methods

Cell culture and reagents

The A549 and H1229 lung cancer cell lines were cultured in Dulbecco's modified Eagle's medium (DMEM, Sigma Aldrich, St Louis, MO, USA) with 5% fetal bovine serum (FBS) [49]. DMH2 and JL5 were synthesized at Rutgers-New Jersey Medical School (Dave Augeri). Z-VAD-FMK and necrostatin-1 were obtained from Sigma-Aldrich, and utilized as per manufacture instructions.

Western blot analysis

Total cellular protein was prepared as previously described and the protein concentration determined using the BCA assay [3]. Protein was separated by SDS-PAGE then transferred to nitrocellulose (Schleicher and Schuell, Keene, NH). The blots were blocked for at least 2 h then incubated overnight at 4 °C with the appropriate primary antibody. Secondary antibodies were applied for 1 h at room temperature. Proteins were detected using the enhanced chemiluminescence system (Amersham, Arlington Heights, IL). The primary antibodies used were rabbit monoclonal anti-pTAK1, rabbit monoclonal XIAP, rabbit monoclonal anti-activated caspase-3, rabbit monoclonal anti-PARP (Cell signaling Technology, Danvers MA), rabbit monoclonal anti-Id1(Calbioreagents, San Mateo, CA), rabbit anti-actin, an affinity isolated antigen specific antibody (Sigma, Saint Louis, MO), and rabbit polyclonal anti-GAPDH (Sigma, St. Louis, MO).

Chemical synthesis of JL5

To synthesize 4-(6-bromopyrazolo[1,5-*a*]pyrimidin-3-yl) quinolone (2 in Supplementary Scheme S1) a solution of 4-(quinolin-4-yl)-1*H*-pyrazol-3-amine (535 mg, 2.54 mmol, 1 eq) in acetic acid (20 ml) was added 2-bromomalonaldehyde (383 mg, 2.54 mmol, 1 eq). After stirring for 16 h at room temperature, the reaction was diluted in water up to 150 ml total solvent. The solution was adjusted to a pH of 5–6 with careful addition of sodium hydroxide when a solid began to precipitate. After 30 min, the suspended solid was subjected to sonication, filtered and washed with water. The solid was recrystallized in MeOH to yield the title compound (752 mg, 91% yield) as a white solid. ^{1}H NMR (500 MHz, DMSO-d_6) 9.77 (d, J = 2.2 Hz, 1H), 8.94 (d, J = 4.5 Hz, 1H), 8.78–8.71 (m, 1H), 8.69 (s, 1H), 8.09 (td, J = 8.3, 1.4 Hz, 2H), 7.78 (ddd, J = 8.2, 6.7, 1.4 Hz, 1H), 7.71 (d, J = 4.4 Hz, 1H), 7.58 (ddd, J = 8.3, 6.8, 1.3 Hz, 1H). MS: 324.75, 326.80 $[M + H]^+$.

To synthesize 4-(3-(4-(4,4,5,5-tetramethyl-1,3,2-dioxaborolan-2-yl)phenyl)propyl)morpholine (3 in Supplementary Scheme S1) a solution of 4-(3-(4-bromophenyl)propyl) morpholine (110 mg, 0.387 mmol, 1 eq), bis(pinacolato) diboron (147 mg, 0.581 mmol, 1.5 eq), $PdCl_2(dppf)CH_2Cl_2$ (16 mg, 0.0194 mmol, 0.05 eq), and KOAc (104 mg, 1.16 mmol, 3 eq) in dioxane (4 ml) was heated in a microwave reactor for 15 min at 130 °C. The crude reaction was diluted in hexanes and filtered over a pad of celite to remove inorganics. The filtrate was purified by silica gel chromatography (50% → 100% EtOAc/Hex) and concentrated to afford the title compound (115 mg, 90%) as an oil that was used in the subsequent coupling without further purification. MS: 332.05 $[M + H]^+$.

To synthesize JL5 (1 in Supplementary Scheme S1) a mixture of 4-(6-bromopyrazolo[1,5-*a*]pyrimidin-3-yl)quinolone (300 mg, 0.810 mmol, 1 eq), 4-(3-(4-(4,4,5,5-tetramethyl-1,3,2-dioxaborolan-2-yl)phenyl)propyl)morpholine (402 mg, 1.22 mmol, 1.5 eq), $PdCl_2(PPh_3)_2$ (28 mg, 0.405 mmol, 0.05 eq) in dioxane (9 ml) and 2 M aqueous Na_2CO_3 (6 ml) was heated in a microwave reactor for 10 min at 130 °C. The reaction was partitioned in EtOAc and water followed by filtration over celite to remove insoluble impurities. The filtered organic was separated and the filtered aqueous was extracted 2× EtOAc. The combined organic was dried over Na_2SO_4, filtered and concentrated. The residue was dissolved in dilute aqueous HCl and washed 2× DCM. The acidic aqueous was made basic with 1 M NaOH and extracted 4× CM. The combined organic was dried over Na_2SO_4, filtered and concentrated. The residue was purified by silica gel chromatography (2% → 5% MeOH/DCM) and product containing fractions were combined and concentrated. Recrystallization from EtOAc afforded the title compound (175 mg, 48%) as a white solid.

Evaluation of genetic abnormalities of BMP signaling in NSCLC

We used The Cancer Genome Atlas (TCGA) database available through cBioportal (http://www.cbioportal.org/public-portal/; accessed on 18 March 2016), a publicly available data portal to investigate the frequency of alterations and expression of the BMP family ligands, receptors, transcription factors, and BMP downstream mediated targets regulating cell survival [50, 51]. Data sets were queried for lung adenocarcinoma and lung squamous cell cancers (provisional for both). Only cases with complete data on mutations, copy-number alterations, and mRNA expression were included. Alterations in BMP signaling in

NSCLC cell lines (CCLE, Cancer Cell Line Encyclopedia) were queried through cBioportal [52]. Dysregulated gene expression was defined by $Z > 2$ (over-expression) or $Z \leq 2$ (reduced expression). Software tools embedded within cBioPortal were used to determine the proportion of samples within each dataset with alterations or up/downregulation.

Cell viability

Lung cancer cells were plated into six-well plates. The following day cells were treated with the BMP inhibitor for the designated amount of time. The live and dead cells were determined using the Vi-CELL cell analyzer (Beckman Coulter). Vi-CELL cell analyzer examined 500 cells per sample and uses utilizes trypan blue dye exclusion to determine the number of dead cells.

Annexin V staining

To assess apoptotic cell death, H1299 cells in six-well plates were treated with DMSO or JL5 2.5 μM for 48 h. Cells were then stained with labeled Annexin V and 7-AAD as per manufacturer's instructions (Thermo Fisher Scientific). Cells were then analyzed by flow cytometry.

IC_{50} kinase assay

IC_{50} assays were performed for alk2, alk3, alk6, alk5, BMPRII, and TGFβ for JL5 and JL12 (Reaction Biology Corporation, Malvern, PA). This was a 10-point assay ranging from 100 μM to 100 nM performed in duplicate with the ATP concentration of 10 μM.

Plasma protein binding

Mouse protein plasma binding for JL5 was performed using equilibrium dialysis (Sai Life Sciences Limited, Pune India).

Metabolic stability

Mouse liver microsomes were treated with DMSO or JL5 for 0.5, 15, 30, and 60 min. The plates were centrifuged and 100 μL aliquots analyzed by liquid chromatography-mass spectrometry (LC-M/MS) (Sai Life Sciences Limited, Pune India).

Pharmacokinetics

The pharmacokinetics of JL5 was examined in BALB/c mice following intravenous and intraperitoneal (i.p.) administration (Sai Life Sciences Limited, Pune India). Blood samples were taken 0.08, 0.25, 0.5, 1, 2, 4, 8, 12, and 24 h and analyzed with LC/MS/MS. Plasma half-life, clearance, AUC, and volume of distribution were then determined (Sai Life Sciences Limited, Pune India).

Luciferase assay

H1299 cells were stably transfected with the Id-1 promoter, which drives the expression of the luciferase reporter. Cells were treated with BMP inhibitors for 48 h then cells lysed and luminescence measured by the TD-20/20 Luminometer (Turner Designs/Turner BioSystems, Sunnyvale, CA) [22].

Humanized and non-humanized tumor xenograft studies

Tumor xenografts from H1299 cells were established by injection of 2 million cells into the intradermal space of the flanks of NOD-*scid* IL2Rgamma^{null} (NSG) mice (bred in-house and randomly assigned to groups without blinding). When tumors reached approximately 4 mm × 4 mm, mice were treated with 3 or 10 mg/kg of JL5 twice daily (or DMSO control) for four days. In some experiment, the NSG mice also received adoptive transfer (via intravenous injection, as previously described [53–55]) of 1–2 million cells donor HLA-compatible human peripheral blood immune cells per mouse and were treated with 10 mg/kg of JL5 twice daily (or DMSO control) for 13 or 21 days, as described for each set of experiments. Tumors were measured using electronic calipers and dissected and processed at the end of each study, as previously described [56–58]. For each experiment, 7–8 mice per group were included (as detailed for each individual experiment) a sample size powered to identify statistical significance with a minimal number of mice. The power calculation applies to the tumor size at the final time point. Experiments were conducted in compliance with ethical regulations and approved by Rutgers IACUC.

Quantifying tumor necrosis

To quantify necrosis H&E-stained slides from each tumor were analyzed using CellSens imaging software (Olympus Life Science). Necrotic and viable tissue areas were manually delineated to calculate percent necrosis.

Toxicity studies

Mice treated with DMSO, 3 mg/kg, and 10 mg/kg of JL5 twice daily for four days were euthanized and postmortem examinations were performed at the scheduled necropsy. At the time of necropsy, lungs, kidneys, and livers were collected and fixed in 10% neutral-buffered formalin. Histomorphological examination of hematoxylin and eosin (H&E)-stained paraffin sections were performed by a board certified veterinary pathologist. Mice in 21-day repeat-dose toxicity studies treated with DMSO (vehicle) or 10 mg/kg of JL5 were examined four times weekly for lethargy, weight loss, and loss of appetite.

Statistical analysis

The means of the control group and treated groups were compared using a two-sided paired Student *t*-test assuming unequal variances. Error bars represent standard error of the mean. A p-value < 0.05 was considered statistically significant.

Supplementary Material

Refer to Web version on PubMed Central for supplementary material.

Acknowledgements

This work utilized shared resources at Rutgers Cancer Institute of New Jersey, which are supported by NCI P30CA72720.

References

1. Sountoulidis A, Stavropoulos A, Giaglis S, Apostolou E, Monteiro R, Chuva de Sousa Lopes SM, et al. Activation of the canonical bone morphogenetic protein (BMP) pathway during lung morphogenesis and adult lung tissue repair. PLoS One. 2012;7:e41460. [PubMed: 22916109]
2. Weaver M, Yingling JM, Dunn NR, Bellusci S, Hogan BL. Bmp signaling regulates proximal-distal differentiation of endoderm in mouse lung development. Development. 1999;126:4005–15. [PubMed: 10457010]
3. Langenfeld EM, Calvano SE, Abou-Nukta F, Lowry SF, Amenta P, Langenfeld J. The mature bone morphogenetic protein-2 is aberrantly expressed in non-small cell lung carcinomas and stimulates tumor growth of A549 cells. Carcinogenesis. 2003;24:1445–54. [PubMed: 12819188]
4. Langenfeld EM, Bojnowski J, Perone J, Langenfeld J. Expression of bone morphogenetic proteins in human lung carcinomas. Ann Thorac Surg. 2005;80:1028–32. [PubMed: 16122479]
5. Lai TH, Fong YC, Fu WM, Yang RS, Tang CH. Osteoblasts-derived BMP-2 enhances the motility of prostate cancer cells via activation of integrins. Prostate. 2008;68:1341–53. [PubMed: 18512729]
6. Clement JH, Raida M, Sanger J, Bicknell R, Liu J, Naumann A, et al. Bone morphogenetic protein 2 (BMP-2) induces in vitro invasion and in vivo hormone independent growth of breast carcinoma cells. Int J Oncol. 2005;27:401–7. [PubMed: 16010421]
7. Owens P, Pickup MW, Novitskiy SV, Giltnane JM, Gorska AE, Hopkins CR, et al. Inhibition of BMP signaling suppresses metastasis in mammary cancer. Oncogene. 2015;34:2437–49. [PubMed: 24998846]
8. Kleeff J, Maruyama H, Ishiwata T, Sawhney H, Friess H, Buchler MW, et al. Bone morphogenetic protein 2 exerts diverse effects on cell growth in vitro and is expressed in human pancreatic cancer in vivo. Gastroenterology. 1999;116:1202–16. [PubMed: 10220513]
9. Rothhammer T, Poser I, Soncin F, Bataille F, Moser M, Bosserhoff AK. Bone morphogenic proteins are overexpressed in malignant melanoma and promote cell invasion and migration. Cancer Res. 2005;65:448–56. [PubMed: 15695386]
10. Nguyen A, Scott MA, Dry SM, James AW. Roles of bone morphogenetic protein signaling in osteosarcoma. Int Orthop. 2014;38:2313–22. [PubMed: 25209345]
11. Langenfeld EM, Langenfeld J. Bone morphogenetic protein-2 stimulates angiogenesis in developing tumors. Mol Cancer Res. 2004;2:141–9. [PubMed: 15037653]
12. Langenfeld EM, Kong Y, Langenfeld J. Bone morphogenetic protein 2 stimulation of tumor growth involves the activation of Smad-1/5. Oncogene. 2006;25:685–92. [PubMed: 16247476]
13. Le Page C, Puiffe ML, Meunier L, Zietarska M, de Ladurantaye M, Tonin PN, et al. BMP-2 signaling in ovarian cancer and its association with poor prognosis. J Ovarian Res. 2009;2:4. [PubMed: 19366455]
14. Ye L, Mason MD, Jiang WG. Bone morphogenetic protein and bone metastasis, implication and therapeutic potential. Front. 2011;16:865–97.
15. Nickel J, Sebald W, Groppe JC, Mueller TD. Intricacies of BMP receptor assembly. Cytokine Growth Factor Rev. 2009;20:367–77. [PubMed: 19926516]
16. Attisano L, Wrana JL. Signal transduction by the TGF-beta superfamily. Sci (New Y, NY). 2002;296:1646–7.
17. Hollnagel A, Oehlmann V, Heymer J, Ruther U, Nordheim A. Id genes are direct targets of bone morphogenetic protein induction in embryonic stem cells. J Biol Chem. 1999;274:19838–45. [PubMed: 10391928]
18. Katagiri T, Imada M, Yanai T, Suda T, Takahashi N, Kamijo R. Identification of a BMP-responsive element in Id1, the gene for inhibition of myogenesis. Genes Cells. 2002;7:949–60. [PubMed: 12296825]
19. Korchynskyi O, ten Dijke P. Identification and functional characterization of distinct critically important bone morphogenetic protein-specific response elements in the Id1 promoter. J Biol Chem. 2002;277:4883–91. [PubMed: 11729207]
20. Kurooka H, Nakahiro T, Mori K, Sano K, Yokota Y. BMP signaling is responsible for serum-induced Id2 expression. Biochem Biophys Res Commun. 2012;420:281–7. [PubMed: 22421219]

21. Lyden D, Young AZ, Zagzag D, Yan W, Gerald W, O'Reilly R, et al. Id1 and Id3 are required for neurogenesis, angiogenesis and vascularization of tumour xenografts. Nature. 1999;401:670–7. [PubMed: 10537105]
22. Augeri DJ, Langenfeld E, Castle M, Gilleran JA, Langenfeld J. Inhibition of BMP and of TGFbeta receptors downregulates expression of XIAP and TAK1 leading to lung cancer cell death. Mol Cancer. 2016;15:27. [PubMed: 27048361]
23. Liu Z, Shen J, Pu K, Katus HA, Ploger F, Tiefenbacher CP, et al. GDF5 and BMP2 inhibit apoptosis via activation of BMPR2 and subsequent stabilization of XIAP. Biochim Biophys Acta. 2009;1793:1819–27. [PubMed: 19782107]
24. Yamaguchi K, Nagai S, Ninomiya-Tsuji J, Nishita M, Tamai K, Irie K, et al. XIAP, a cellular member of the inhibitor of apoptosis protein family, links the receptors to TAB1-TAK1 in the BMP signaling pathway. EMBO J. 1999;18:179–87. [PubMed: 9878061]
25. Obexer P, Ausserlechner MJ. X-linked inhibitor of apoptosis protein—a critical death resistance regulator and therapeutic target for personalized cancer therapy. Front Oncol. 2014;4:197. [PubMed: 25120954]
26. Kaufmann T, Strasser A, Jost PJ. Fas death receptor signalling: roles of Bid and XIAP. Cell Death Differ. 2012;19:42–50. [PubMed: 21959933]
27. Mihaly SR, Ninomiya-Tsuji J, Morioka S. TAK1 control of cell death. Cell Death Differ. 2014;21:1667–76. [PubMed: 25146924]
28. Vanlangenakker N, Vanden Berghe T, Bogaert P, Laukens B, Zobel K, Deshayes K, et al. cIAP1 and TAK1 protect cells from TNF-induced necrosis by preventing RIP1/RIP3-dependent reactive oxygen species production. Cell Death Differ. 2011;18:656–65. [PubMed: 21052097]
29. Zon LI, Peterson RT. In vivo drug discovery in the zebrafish. Nat Rev Drug Discov. 2005;4:35–44. [PubMed: 15688071]
30. Hao J, Ho JN, Lewis JA, Karim KA, Daniels RN, Gentry PR, et al. In vivo structure-activity relationship study of dorsomorphin analogues identifies selective VEGF and BMP inhibitors. ACS Chem Biol. 2010;5:245–53. [PubMed: 20020776]
31. Yu PB, Deng DY, Lai CS, Hong CC, Cuny GD, Bouxsein ML, et al. BMP type I receptor inhibition reduces heterotopic [corrected] ossification. Nat Med. 2008;14:1363–9. [PubMed: 19029982]
32. Balboni AL, Hutchinson JA, DeCastro AJ, Cherukuri P, Liby K, Sporn MB, et al. DeltaNp63alpha-mediated activation of bone morphogenetic protein signaling governs stem cell activity and plasticity in normal and malignant mammary epithelial cells. Cancer Res. 2013;73:1020–30. [PubMed: 23243027]
33. Martinez VG, Hernandez-Lopez C, Valencia J, Hidalgo L, Entrena A, Zapata AG, et al. The canonical BMP signaling pathway is involved in human monocyte-derived dendritic cell maturation. Immunol Cell Biol. 2011;89:610–8. [PubMed: 21102536]
34. Martinez VG, Sacedon R, Hidalgo L, Valencia J, Fernandez-Sevilla LM, Hernandez-Lopez C, et al. The BMP pathway participates in human naive CD4+ T cell activation and homeostasis. PloS One. 2015;10:e0131453. [PubMed: 26110906]
35. Robson NC, Hidalgo L, McAlpine T, Wei H, Martinez VG, Entrena A, et al. Optimal effector functions in human natural killer cells rely upon autocrine bone morphogenetic protein signaling. Cancer Res. 2014;74:5019–31. [PubMed: 25038228]
36. Yu PB, Hong CC, Sachidanandan C, Babitt JL, Deng DY, Hoyng SA, et al. Dorsomorphin inhibits BMP signals required for embryogenesis and iron metabolism. Nat Chem Biol. 2008;4:33–41. [PubMed: 18026094]
37. Cuny GD, Yu PB, Laha JK, Xing X, Liu JF, Lai CS, et al. Structure-activity relationship study of bone morphogenetic protein (BMP) signaling inhibitors. Bioorg Med Chem Lett. 2008;18:4388–92. [PubMed: 18621530]
38. Pao W, Miller V, Zakowski M, Doherty J, Politi K, Sarkaria I, et al. EGF receptor gene mutations are common in lung cancers from "never smokers" and are associated with sensitivity of tumors to gefitinib and erlotinib. Proc Natl Acad Sci USA. 2004;101:13306–11. [PubMed: 15329413]
39. Zhou W, Ercan D, Chen L, Yun CH, Li D, Capelletti M, et al. Novel mutant-selective EGFR kinase inhibitors against EGFR T790M. Nature. 2009;462:1070–4. [PubMed: 20033049]

40. Langenfeld E, Hong CC, Lanke G, Langenfeld J. Bone morphogenetic protein type I receptor antagonists decrease growth and induce cell death of lung cancer cell lines. PLoS One. 2013;8: e61256. [PubMed: 23593444]
41. Hao J, Lee R, Chang A, Fan J, Labib C, Parsa C, et al. DMH1, a small molecule inhibitor of BMP type i receptors, suppresses growth and invasion of lung cancer. PloS One. 2014;9:e90748. [PubMed: 24603907]
42. Dohi T, Okada K, Xia F, Wilford CE, Samuel T, Welsh K, et al. An IAP-IAP complex inhibits apoptosis. J Biol Chem. 2004;279:34087–90. [PubMed: 15218035]
43. de Bruin EC, Medema JP. Apoptosis and non-apoptotic deaths in cancer development and treatment response. Cancer Treat Rev. 2008;34:737–49. [PubMed: 18722718]
44. Galban S, Hwang C, Rumble JM, Oetjen KA, Wright CW, Boudreault A, et al. Cytoprotective effects of IAPs revealed by a small molecule antagonist. Biochem J. 2009;417:765–71. [PubMed: 18851715]
45. Martinez VG, Hidalgo L, Valencia J, Hernandez-Lopez C, Entrena A, del Amo BG, et al. Autocrine activation of canonical BMP signaling regulates PD-L1 and PD-L2 expression in human dendritic cells. Eur J Immunol. 2014;44:1031–8. [PubMed: 24532425]
46. Bobbio A, Alifano M. Immune therapy of non-small cell lung cancer. The future. Pharmacol Res. 2015;99:217–22. [PubMed: 26141705]
47. Sharma P, Allison JP. The future of immune checkpoint therapy. Sci (New Y, NY). 2015;348:56–61.
48. Taube JM, Klein A, Brahmer JR, Xu H, Pan X, Kim JH, et al. Association of PD-1, PD-1 ligands, and other features of the tumor immune microenvironment with response to anti-PD-1 therapy. Clinical cancer research: an official journal of the American Association for. Cancer Res. 2014;20:5064–74.
49. Langenfeld EM, Kong Y, Langenfeld J. Bone morphogenetic protein-2-induced transformation involves the activation of mammalian target of rapamycin. Mol Cancer Res. 2005;3:679–84. [PubMed: 16380505]
50. Cerami E, Gao J, Dogrusoz U, Gross BE, Sumer SO, Aksoy BA, et al. The cBio cancer genomics portal: an open platform for exploring multidimensional cancer genomics data. Cancer Discov. 2012;2:401–4. [PubMed: 22588877]
51. Gao J, Aksoy BA, Dogrusoz U, Dresdner G, Gross B, Sumer SO, et al. Integrative analysis of complex cancer genomics and clinical profiles using the cBioPortal. Sci Signal. 2013;6:pl1.
52. Barretina J, Caponigro G, Stransky N, Venkatesan K, Margolin AA, Kim S, et al. The Cancer Cell Line Encyclopedia enables predictive modelling of anticancer drug sensitivity. Nature. 2012;483:603–7. [PubMed: 22460905]
53. Hahm E, Wei C, Fernandez I, Li J, Tardi NJ, Tracy M, et al. Bone marrow-derived immature myeloid cells are a main source of circulating suPAR contributing to proteinuric kidney disease. Nat Med. 2017;23:100–6. [PubMed: 27941791]
54. Lu R, Wu S, Zhang Y, Xia Y, Huelsmann EJ, Lacek AT, et al. HIV infection accelerates gastrointestinal tumor outgrowth in NSG-HuPBL mice. AIDS Res Hum Retrovir. 2014;30:677–84. [PubMed: 24593860]
55. Zhang YG, Wu S, Lu R, Richards MH, Huelsmann EJ, Lacek AT, et al. HIV infection leads to redistribution of leaky claudin-2 in the intestine of humanized SCID IL-2R(−/−) Hu-PBMC mice. AIDS Res Hum Retrovir. 2015;31:774–5. [PubMed: 25853489]
56. Kohlhapp FJ, Broucek JR, Hughes T, Huelsmann EJ, Lusciks J, Zayas JP, et al. NK cells and CD8+ T cells cooperate to improve therapeutic responses in melanoma treated with interleukin-2 (IL-2) and CTLA-4 blockade. J Immunother. Cancer 2015;3:18. [PubMed: 25992289]
57. Kohlhapp FJ, Huelsmann EJ, Lacek AT, Schenkel JM, Lusciks J, Broucek JR, et al. Non-oncogenic acute viral infections disrupt anti-cancer responses and lead to accelerated cancer-specific host death. Cell Rep. 2016;17:957–65. [PubMed: 27760326]
58. Zloza A, Kohlhapp FJ, Lyons GE, Schenkel JM, Moore TV, Lacek AT, et al. NKG2D signaling on CD8(+) T cells represses T-bet and rescues CD4-unhelped CD8(+) T cell memory recall but not effector responses. Nat Med. 2012;18:422–8. [PubMed: 22366950]

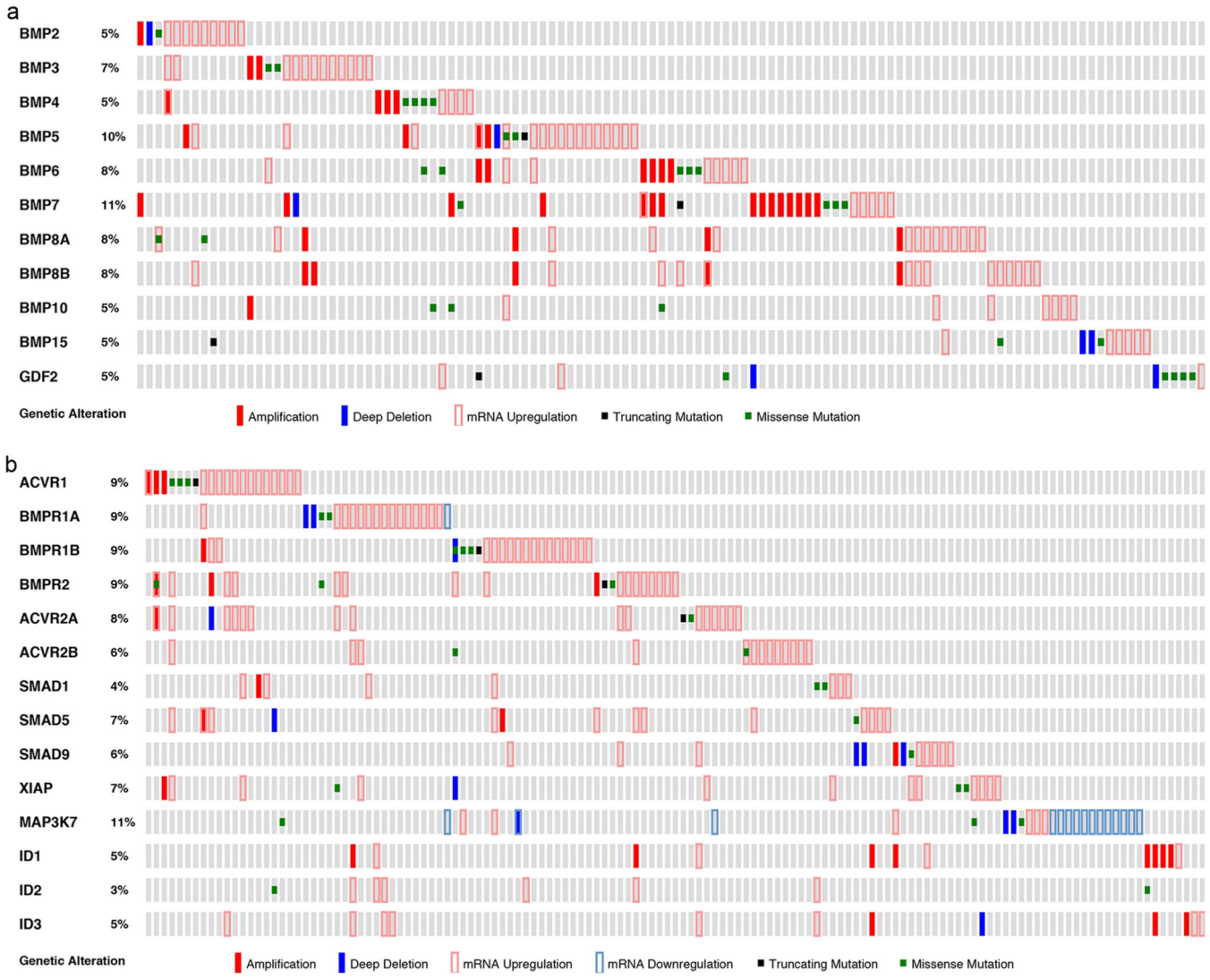

Fig. 1.

Genetic alterations of the BMP signaling cascade are infrequent in lung adenocarcinomas. The TCGA database was queried for DNA amplifications, deep deletions, truncating mutations, missense mutations, and mRNA expression of (**a**) BMP ligands in lung adenocarcinomas ($n = 117$) and (**b**) BMP receptors, BMP transcription factors (Smad-1/5/9), and BMP downstream targets (XIAP, MAP3K7/TAK1, ID1, ID2, ID3) in lung adenocarcinomas ($n = 135$). Gray boxes indicate gene expression without alteration

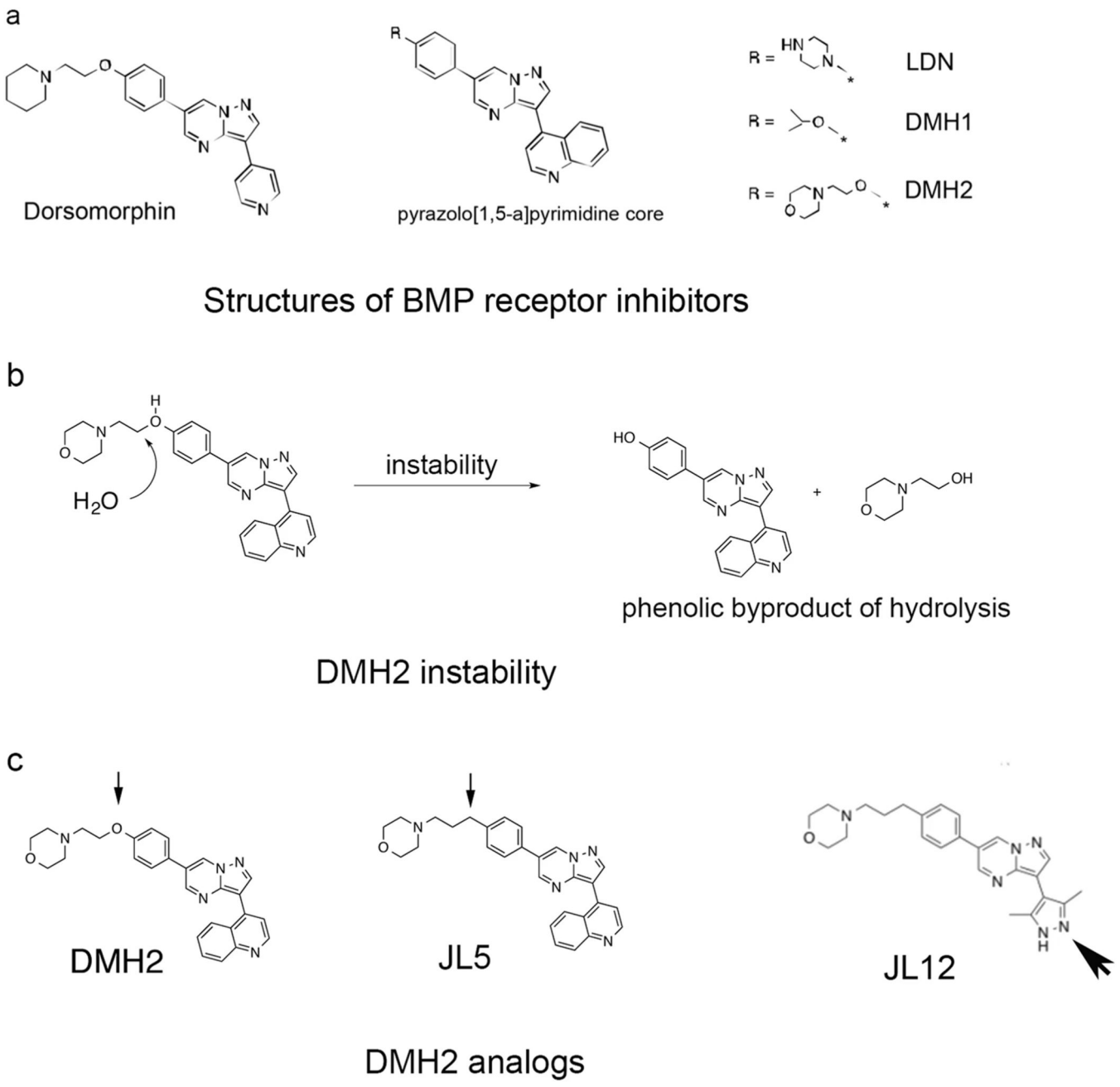

Fig. 2.

A carbon for oxygen substitution to DMH2 results in the formation of JL5. **a** Structures of Dorsomorphin analogs, which were derived from the same pyrazolo[1,5-a] pyrimidine core. BMP inhibitors DMH2, DMH1, and LDN differ in the substitutions made at the R position of the pyrazolo[1,5-a] pyrimidine core. **b** DMH2 was found to be chemically and metabolically unstable. LCMS of a sample of stored DMH2 for 4 months revealed the phenolic byproduct due to morpholine side-chain hydrolysis. **c** Structure of DMH2 analogs JL5 and the inactive analog JL12. The small arrowhead shows the carbon substitution for

oxygen in the DMH2 side chain to create JL5. The large arrowhead shows the imidapyrazole substitution made to JL5 to create JL12

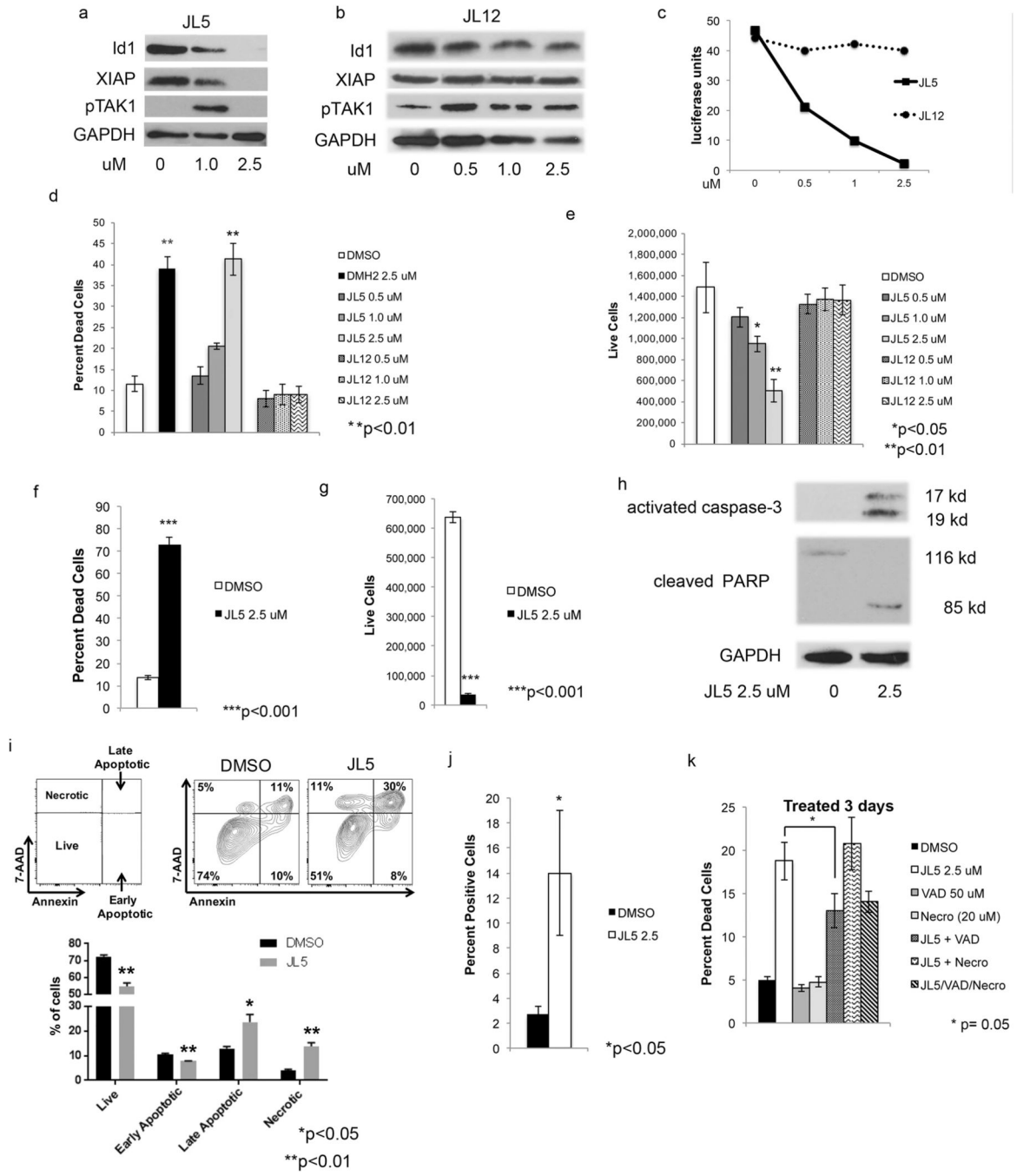

Fig. 3.

JL5 but not JL12 regulates BMP signaling and induces cell death. **a, b** Western blot analyses of H1299 cells treated with JL5 or JL12 for 72 h showing that JL5 but not JL12 decreases expression of Id1, XIAP, and pTAK1. **c** H1299 cells stably expressing the Id1-luciferase reporter were treated with JL5 and JL12 for 48 h. JL5 but not JL12 decreases the activity of the Id1 promoter. **d, e** H1299 cells were treated with JL5 or JL12 for 72 h and (**d**) the percent dead and (**e**) the number of live cells determined. **f, g** H1299 cells were treated with JL5 for 7 days and the percent dead and number of live cells determined. **h** Western

blot analysis of H1299 cells treated with JL5 for 3 days demonstrating that JL5 activates caspase-3 and cleaves PARP. **i** H1299 cells were treated with JL5 2.5 μM for 48 h. Cells were stained were then stained with fluorescently labeled Annexin V and 7-AAD and analyzed by flow cytometry. JL5 induced both late stage apoptosis and necrotic cell death. **j** TUNEL assay of H1299 cells treated with JL5 for 24 h demonstrating an increase in DNA double-stranded breaks. **k** H1299 cells were pretreated with Z-VAD-FMK (VAD) or necrostatin for 1 h then treated with DMSO or JL5 for 3 days and percent death cells determined. VAD but not necrostatin partially inhibited cell death induced by JL5. All experiments were performed at least 3 times with similar results except (**c**), which was performed twice with similar results

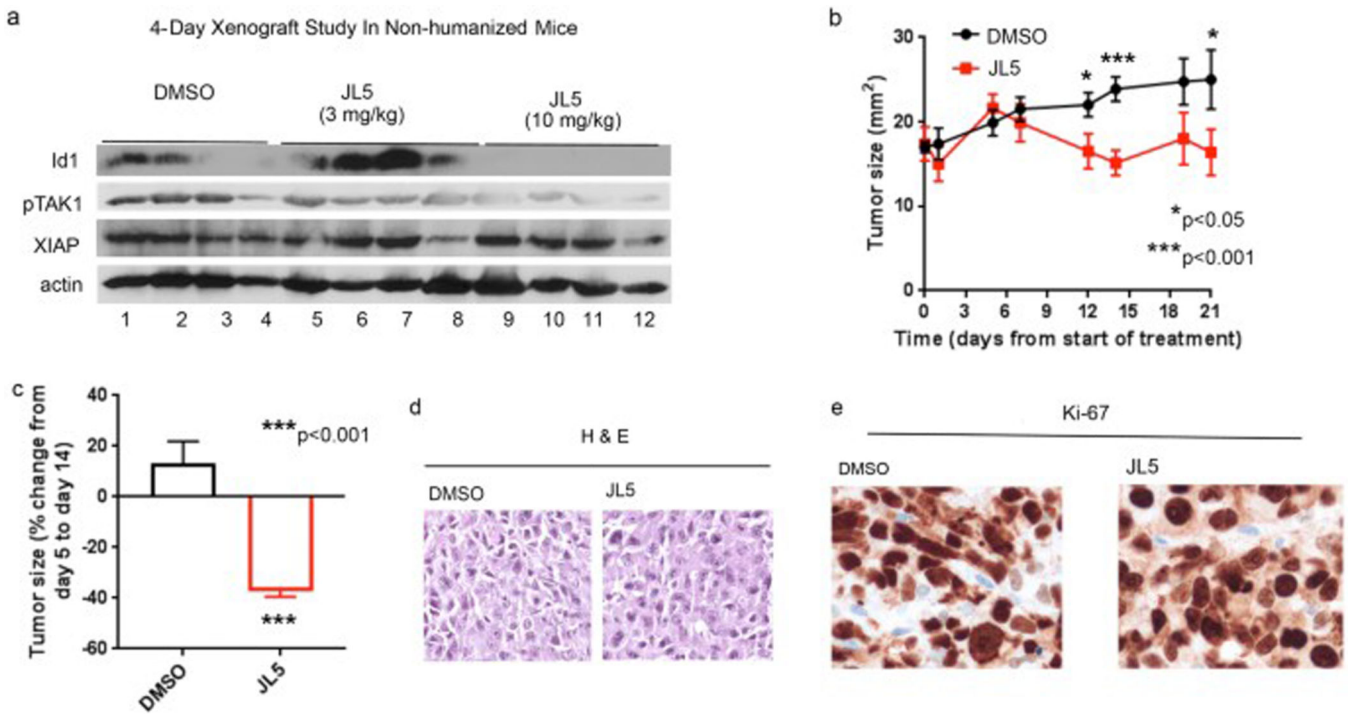

Fig. 4.

JL5 suppresses BMP signaling and decreases growth of tumor xenografts in NSG mice without immune cells. **a** Western blot analysis of H1299 tumors in NSG mice without immune cells treated with JL5 for 4 days. **b–e** H1299 cells were injected intradermally into the flanks of NSG mice. Five days later after tumors had reached ~5 mm^2 mice were treated with DMSO or 10 mg/kg JL5 (twice daily) (n = 8 mice for each group) for 21 days. Growth curves of tumors treated for 21 days (**b**). Fold change in tumor growth from day 5 post-treatment to day 14 (**c**). DMSO-treated tumors increased in size while JL5-treated tumors demonstrate tumor regression. H&E staining of tumors shows no significant differences in the cell death (**d**) and IHC for the proliferation marker Ki67 on treatment day 21 show no significant differences between groups (**e**)

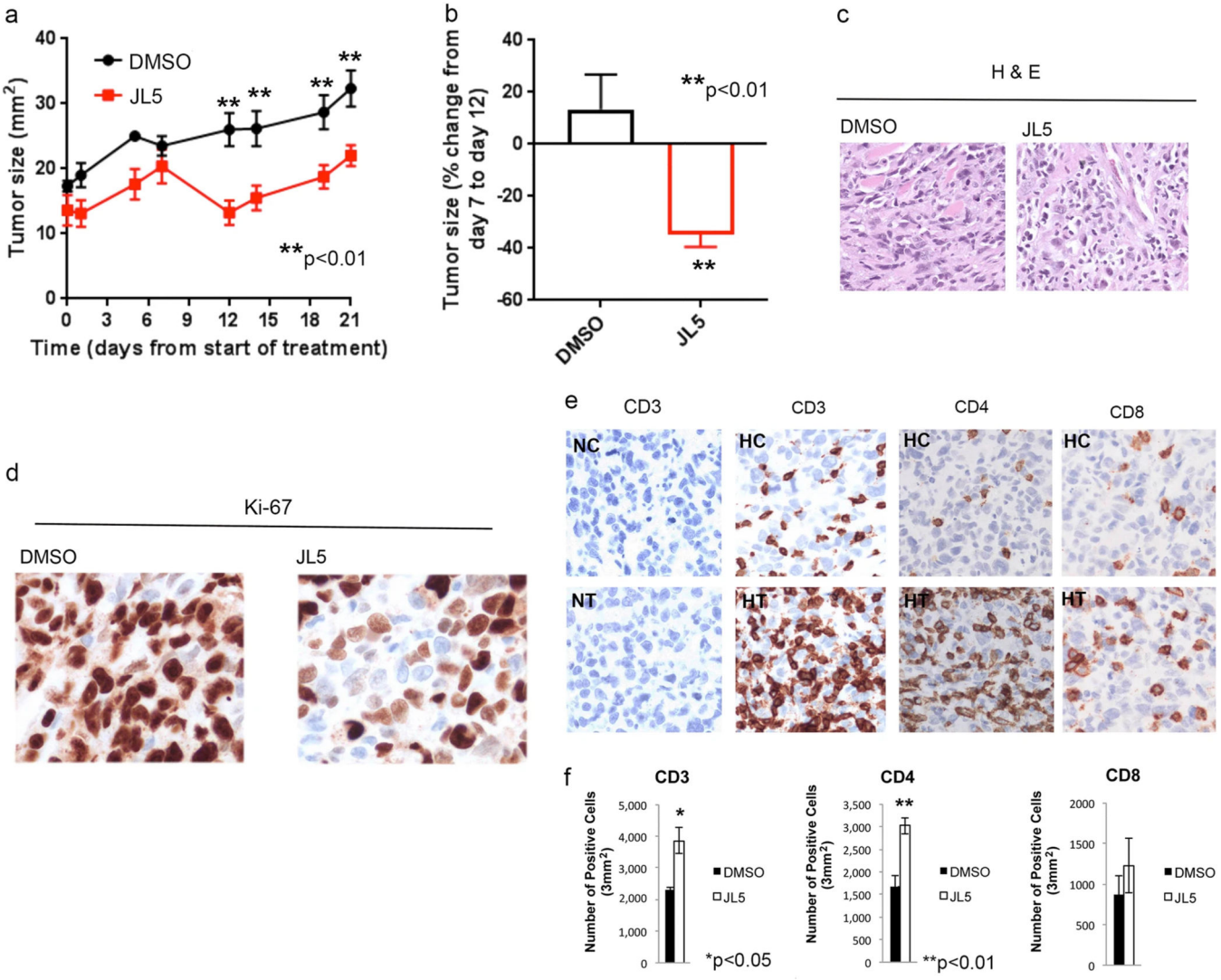

Fig. 5.

JL5 suppresses growth of tumor xenografts in NSG mice with immune cells and induces infiltration of immune cells. **a–e** NSG mice received adoptively transferred human immune cells and then H1299 cells were injected intradermally into the flanks. Five days later after tumors had reached ~5 mm^2 mice were treated with DMSO or 10 mg/kg JL5 (twice daily) (n = 8 mice for each group) for 21 days. Growth curves of tumors treated for 21 days (**a**). Percent change in tumor growth from day 7 post-treatment to day 12 (**b**). DMSO-treated tumors increase in size while JL5-treated tumors demonstrate tumor regression. H&E staining of tumors shows no significant differences in the number of death cells (**c**). IHC for the proliferation marker Ki67 on treatement day 21 demonstrates a significant decrease in proliferation in tumors treated with JL5 (**d**). IHC staining of tumors on treatment day 21 shows that JL5 increases the number of immune cells within the tumor microenvironment (**e**). Tumors formed in mice that did not receive immune cells were used as controls. NC and NT = non-humanized mice treated with DMSO control or JL5, respectively. HC and HT = humanized mice treated with DMSO control or JL5, respectively. **f** IHC slides were scanned

and the mean number of immune cells quantified using imaging software ($n = 3$ in each group)

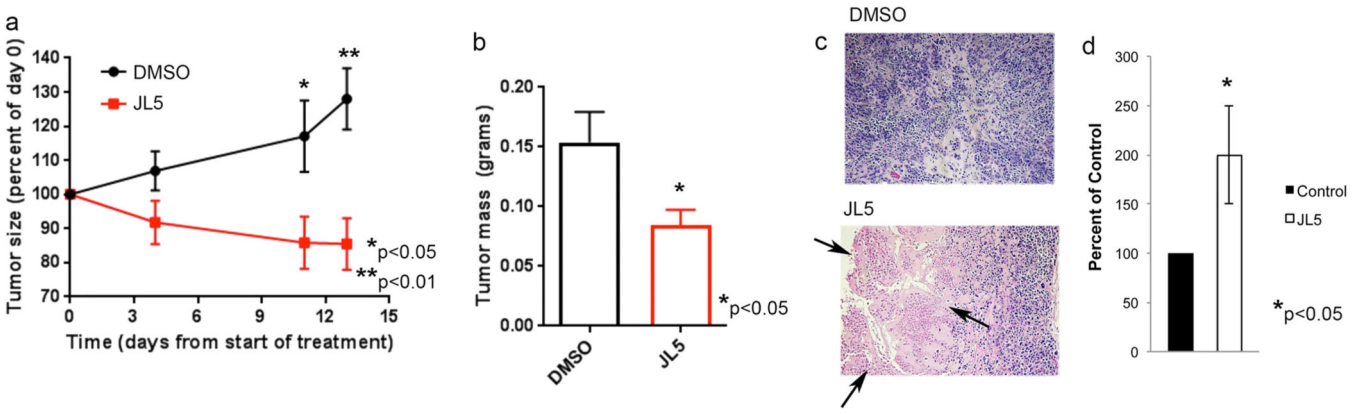

Fig. 6.

JL5 induces death of cancer cells on treatment day 13. NSG mice received adoptively transferred human immune cells and then H1299 cells were injected intradermally into the flanks. Five days later after tumors had reached ~5 mm^2 mice were treated with DMSO or 10 mg/kg JL5 (twice daily) (n = 7 mice for each group) for 13 days. **a, b** Growth curves of tumors (**a**) and tumor weights of xenograft tumors on treatment day 13 (**b**). **c** H&E staining demonstrating significantly more cell death of cancer cells (pink cells shown by arrows) of tumors treated with JL5. **d** The H&E slides were scanned and the percentage of dead cells within each tumor determined using imaging software. Data represents the mean of 7 tumors depicted as the percent of control

Table 1

In vitro PK parameters

Parameter	DMH2	JL5
$Clearance_{INT}$ (mL/min/kg)	250	129
Plasma protein binding	98.60%	98.30%

From: Novel bone morphogenetic protein receptor inhibitor JL5 suppresses tumor cell survival signaling and induces regression of human lung cancer

Table 2

Pharmocokinetics

Compound	Route	C_0/C_{max} (ng/mL)	AUC_{last} (hr×ng/mL)	AUC_{inf} (hr×ng/mL)	$T_{1/2}$ (hr)	CL (mL/min/kg)	Vss (L/kg)
DMH2[(2)]	i.v.	3,035	485	487	0.95	68	0.95
	p.o.	684	707	729	—	—	—
JL5	i.v.	568	349	381	0.57	194	8.78
	p.o.	1,282	1,605	1,645	—	—	—

From: Novel bone morphogenetic protein receptor inhibitor JL5 suppresses tumor cell survival signaling and induces regression of human lung cancer

Table 3

Receptor kinase inhibition

Compound	IC50 (nM)					
	ALK2/ACVR1	ALK3/BMPR1A	ALK6/BMPR1B	BMPR2	ALK5/TGFβR1	TGFβR2
DMH2[(2)]	23	92	43	7,950	1690	193
JL5	1	<5	2	8,510	440	40
JL12	2,690	8,690	9,310	>10,000	—	3,670

From: Novel bone morphogenetic protein receptor inhibitor JL5 suppresses tumor cell survival signaling and induces regression of human lung cancer